Optimized perturbation theory at finite temperature

S. Chiku
Institute of Physics, University of Tsukuba, Tsukuba, Ibaraki 305, Japan
and Yukawa Institute for Theoretical Physics, Kyoto University, Kyoto 606, Japan

T. Hatsuda
Institute of Physics, University of Tsukuba, Tsukuba, Ibaraki 305, Japan
and Physics Department, Kyoto University, Kyoto 606, Japan
(Received 3 March 1998; published 20 August 1998)

An optimized perturbation theory (OPT) at finite temperature T, which resums higher order terms in the naive perturbation, is developed in $O(N)$ ϕ^4 theory. It is proved that (i) the renormalization of the ultraviolet divergences can be carried out systematically in any given order of OPT and (ii) the Nambu-Goldstone theorem is satisfied for arbitrary N and for any given order of OPT. The method is applied for the $O(4)$ σ model to study the soft modes associated with the chiral transition in quantum chromodynamics. Threshold enhancement of the spectral functions at finite T in the scalar and pseudoscalar channels is shown to be a typical signal of the chiral transition. [S0556-2821(98)04617-7]

PACS number(s): 11.10.Wx, 11.30.Rd, 12.38.Cy, 12.38.Mh

I. INTRODUCTION

One of the main goals of the ultrarelativistic heavy-ion experiments planned at the BNL Relativistic Heavy Ion Collider (RHIC) and CERN Large Hadron Collider (LHC) [1] is to observe the structural change of the ground state of quantum chromodynamics (QCD) at finite temperature (T), namely, the phase transition to the quark-gluon plasma. The numerical simulation based on lattice QCD is a powerful tool to study the static nature of this phase transition, in which the critical temperature and the critical exponents are actively studied [2]. In particular, there exists numerical evidence that the chiral transition for massless two flavors is of second order, although the case for the real world (two light quarks + one medium-heavy quark) is not settled yet [3].

If the phase transition is of second order or is close to it, there arises long range fluctuations in both spatial and temporal (real-time) directions. The latter is usually called the soft mode and has been used as a probe to study phase transitions of solid states and condensed matter [4].

Despite the experimental significance of the soft modes in QCD, lattice QCD simulations cannot treat such real-time modes in a straightforward manner. This is why effective theories of QCD have been adopted to study time-dependent phenomena (see the reviews in [5,6] and references cited therein). However, even in tractable effective theories such as the linear σ model, there exist subtleties at finite T. In fact, the necessity of the resummation of higher order terms in perturbative expansions both at high T and low T has been known for a long time [7,8]. Also, the renormalization of the ultraviolet (UV) divergences and related issues in resumed perturbation theories have been discussed in the literature especially for theories with spontaneous symmetry breaking (SSB) [9].

Recently, we have reported our analysis of a particular resummation method and its application to the soft modes in QCD [10]. The present paper contains not only a detailed description of our previous analysis but also further investigations.

The purpose of the present paper is twofold. First, we will develop an improved loop-wise expansion at finite T. Our starting point is optimized perturbation theory (OPT) (or sometimes called delta expansion, variational perturbation theory, etc.) which is a generalization of the mean-field method [11] and is known to work in various quantum systems [12]. Its application to field theory at finite T has been considered in Refs. [13,14] for the first time. We will further develop the idea and prove the renormalizability and the Nambu-Goldstone (NG) theorem in $O(N)$ ϕ^4 theory at finite T order by order in OPT. Our second purpose is to study the soft modes associated with the chiral transition in QCD by taking into account interactions among the soft modes (mode couplings). The use of OPT is essential for this purpose, which will be demonstrated using the $O(4)$ σ model.

The organization of this paper is as follows. In Sec. II, we introduce a loop-wise expansion on the basis of OPT. The renormalization of UV divergences and the realization of the NG theorem in this method are also discussed. In Sec. III, we will apply the OPT developed in Sec. II for the $O(4)$ σ model to study the spectral functions of the σ meson and the π meson at $T \neq 0$. The detectability of the soft modes by the diphoton process $\sigma \rightarrow 2\gamma$ in hot hadronic matter is also examined. Section IV is devoted to a summary and concluding remarks.

II. OPTIMIZED PERTURBATION AT $T \neq 0$

A. Necessity of resummation at finite T

It has been known that naive perturbations either by a coupling constant or by number of loops break down at $T \neq 0$, and a proper resummation of higher orders is necessary [7]. In fact, no matter what small dimensionless coupling (say, λ) seems to control the perturbative expansion, the powers of T compensate the powers of λ, which invalidates the naive expansion.

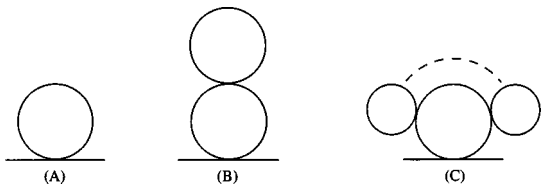

FIG. 1. Bubble and cactus diagrams.

This is easily illustrated in ϕ^4 theory:

$$\mathcal{L}=\frac{1}{2}[(\partial\phi)^2-\mu^2\phi^2]-\frac{\lambda}{4!}\phi^4. \tag{1}$$

Let us first consider the case $\mu^2>0$. The lowest order self-energy diagram Fig. 1(A) is $O(\lambda T^2)$ at high T. However, Fig. 1(B) is $O(\lambda T^2\times\lambda T/\mu)$. Furthermore, higher powers of T/μ arise in higher loops; e.g., the n-loop diagram in Fig. 1(C) is $O(\lambda^n T^{2n-1}/\mu^{2n-3})$. Thus, one should at least resum cactus diagrams to get sensible results at high T [7,15]. Physics behind this resummation is of course the Debye screening mass in the hot plasma.

The naive loop expansion breaks down also for $\mu^2<0$. The tree-level mass m_0 in this case is defined as

$$m_0^2=\mu^2+\frac{\lambda}{2}\xi^2(T), \tag{2}$$

where $\xi(T)$ is the thermal expectation value of ϕ. Since μ^2 is negative and ξ^2 decreases as T increases, m_0^2 becomes tachyonic even below the critical temperature T_c. Therefore, the naive loop expansion using the tree-level propagator ceases to work even before the symmetry restoration takes place, and a proper resummation of higher loop diagrams is necessary [8]. Note that, for $T<T_c$, there is no reason to believe that only the cactus diagrams shown in Fig. 1 are dominant; there exists a three-point vertex $\lambda\xi\phi^3$ which is not negligible for $T\sim\xi(T)$.

B. Resummation method

For theories without SSB, a systematic resummation method to obtain a sensible ''weak-coupling'' expansion at high T was formulated and applied to gauge theory and ϕ^4 theory successfully [16].

For theories with SSB, however, the loop expansion rather than the weak-coupling expansion is relevant, since one needs to treat the thermal effective potential or the Gibbs free energy. We find that optimized perturbation theory, which was applied to finite T system in [13,14], can be formulated in such a way that an improved loop expansion is carried out systematically. Also, the method leads to a transparent renormalization procedure and guarantees the Nambu-Goldstone theorem order by order in the improved loop expansion.

In the following, we divide our resummation procedure into three steps and apply it to ϕ^4 theory. The case for $O(N)$ ϕ^4 theory will be discussed in Sec. II E.

Step 1. Start with a renormalized Lagrangian with counterterms

$$\mathcal{L}(\phi;\mu^2)=\frac{1}{2}[(\partial\phi)^2-\mu^2\phi^2]-\frac{\lambda}{4!}\phi^4 + \frac{1}{2}A(\partial\phi)^2-\frac{1}{2}B\mu^2\phi^2-\frac{\lambda}{4!}C\phi^4+D\mu^4. \tag{3}$$

Here we have explicitly written the argument μ^2 in $\mathcal{L}$ for later use. The mass-independent renormalization scheme with dimensional regularization is assumed in Eq. (3). Just for notational simplicity, the factor $\kappa^{(4-n)}$ to be multiplied to λ is omitted (κ is the renormalization point and n is the number of dimensions). In the actual calculations below, we take the modified minimal subtraction ($\overline{\mathrm{MS}}$) scheme.

The c-number counterterm $D\mu^4$, which was not considered in [14], is necessary to make the thermal effective potential finite. Also, it plays a crucial role for renormalization in OPT as will be shown in Sec. II D.

The thermal effective action $\Gamma[\varphi^2]$ is written as the Euclidean functional integral [17]

$$\Gamma[\varphi^2]=\ln\int[d\phi]\exp\left[\frac{1}{\delta}\int_0^{1/T}d^4x[\mathcal{L}(\phi+\varphi;\mu^2)+J\phi]\right], \tag{4}$$

where $J\equiv-\partial\Gamma[\varphi]/\partial\varphi$ and $\int_0^{1/T}d^4x\equiv\int_0^{1/T}d\tau\int d^3x$. The ''naive'' loop expansion at $T\neq0$ is defined as an expansion by δ [18] with the tree-level mass $\mu^2+\lambda\varphi^2/2$.

Under the naive loop expansion with Eq. (3) for $\mu^2>0$, one can completely fix the renormalization constants. Since ultraviolet divergences do not depend on T in the naive loop expansion [19], A, B, C, and D are independent of T, and are expanded as

$$\begin{pmatrix}A\\B\\C\\D\end{pmatrix}=\sum_{l=1}^{\infty}\begin{pmatrix}a_l\\b_l\\c_l\\d_l\end{pmatrix}\delta^l. \tag{5}$$

The coefficients (a_l,b_l,c_l,d_l) are independent of μ^2, since we use the mass-independent renormalization scheme. Also, the UV divergences in the symmetry-broken phase ($\mu^2<0$) can be removed by the same counterterms determined for $\mu^2>0$ [20,21].

The relations of A,B,C, and D with the standard renormalization constants are $A=Z-1$, $B=Z_\mu Z-1$, and $C=Z_\lambda Z^2-1$, where Z's are defined by $\phi_0=\sqrt{Z}\phi$, $\lambda_0=Z_\lambda\lambda$, and $\mu_0^2=Z_\mu\mu^2$, with suffix 0 indicating unrenormalized quantities.

Step 2. Rewrite the Lagrangian (3) by introducing a new mass parameter m^2 following the idea of OPT [12]:

$$\mu^2=m^2-(m^2-\mu^2)\equiv m^2-\chi. \tag{6}$$

This identity should be used not only in the standard mass term but also in the counterterms [22], which is crucial to show the order by order renormalization in OPT:

$$\mathcal{L}(\phi;\mu^2)=\mathcal{L}_{\rm r}+\mathcal{L}_{\rm c} \tag{7}$$

$$\mathcal{L}_{\rm r}=\frac{1}{2}[(\partial\phi)^2-m^2\phi^2]-\frac{\lambda}{4!}\phi^4+\frac{1}{2}\chi\phi^2 \tag{8}$$

$$\mathcal{L}_{\rm c}=\frac{1}{2}A(\partial\phi)^2-\frac{1}{2}B(m^2-\chi)\phi^2 - \frac{\lambda}{4!}C\phi^4+D(m^2-\chi)^2. \tag{9}$$

A, B, C, and D in $\mathcal{L}_{\rm c}$ were already determined in step 1.

On the basis of Eq. (7), we define a ''modified'' loop expansion in which the tree-level propagator has a mass $m^2+\lambda\varphi^2/2$ instead of $\mu^2+\lambda\varphi^2/2$. The major difference between this expansion and the naive one is the following assignment:

$$m^2=O(\delta^0),\quad \chi=O(\delta). \tag{10}$$

The physical reason behind this assignment is the fact that χ reflects the effect of interactions. If one adopts an assignment $m^2=O(\delta^0),\chi=O(\delta^0)$, the modified loop expansion immediately reduces to the naive one.

As will be shown explicitly in Sec. II D, all the UV divergences in the modified loop expansion are removed by the counterterms determined in the naive loop expansion.

Since Eq. (7) is simply a reorganization of the Lagrangian, any Green's functions (or its generating functional) calculated in the modified loop expansion should not depend on the arbitrary mass m if they are calculated in all orders. However, one needs to truncate perturbation series at a certain order in practice. This inevitably introduces an explicit m dependence in Green's functions. Procedures to determine m are given in step 3 below.

To find the ground state of the system, one should look for the stationary point of the thermal effective potential $V(\varphi^2)$ defined by

$$V(\varphi^2)=-\frac{\Gamma[\varphi^2=\text{const}]}{\int_0^{1/T}d^4x}. \tag{11}$$

As mentioned above, V calculated up to Lth loops $V_L(\varphi^2;m)$ has an explicit m dependence. Thus the stationary condition reads

$$\frac{\partial V_L(\varphi^2;m)}{\partial\varphi}=0, \tag{12}$$

where the derivative with respect to φ does not act on m by definition. Equation (12) gives a stationary point of V_L for given m.

One may generalize step 2 by adding and subtracting $\alpha_0(\partial_0\phi)^2$, $\alpha_1(\partial_i\phi)^2$, and $\gamma\phi^4$ [23] with α_0, α_1, and γ being finite parameters to be determined by the principle of minimal sensitivity (PMS) or fastest apparent convergence (FAC) conditions (see step 3). α_0 and α_1 are especially important for theories with fermions at finite T and chemical potential [24]. We will, however, concentrate on the simplest version ($\alpha_{0,1}=\gamma=0$) in the following discussions.

Step 3. The final step is to find an optimal value of m by imposing physical conditions in the manner of Stevenson [25] such as the following.

(a) The PMS: this condition requires that a chosen quantity calculated up to Lth loops ($\mathcal{O}_L$) should be stationary by the variation of m:

$$\frac{\partial\mathcal{O}_L}{\partial m}=0. \tag{13}$$

(b) The criterion of the FAC: this condition requires that the perturbative corrections in O_L should be as small as possible for a suitable value of m:

$$\mathcal{O}_L-\mathcal{O}_{L-n}=0, \tag{14}$$

where n is chosen in the range $1\leqslant n\leqslant L$.

The above conditions reduce to self-consistent gap equations whose solution determines the optimal parameter m for a given L. Thus m becomes a nontrivial function of φ, λ, and T [26]. This together with the solution of Eq. (12) completely determines the thermal expectation value $\xi(T)\equiv\langle\phi\rangle$ as well as the optimal parameter $m(T)$. Through this self-consistent process, higher order terms in the naive loop expansion are resumed.

The choice of $\mathcal{O}_L$ in step 3 depends on the quantity one needs to improve most. To study the static nature of the phase transition, the thermal effective potential $V_L(\varphi^2;m)$ is most relevant. Applying the PMS condition for V_L reads

$$\frac{\partial V_L(\varphi^2;m)}{\partial m}=0, \tag{15}$$

which gives a solution $m=m(\varphi)$. This can be used to improve the effective potential at finite T [13]:

$$V_L(\varphi^2;m)\to V_L(\varphi^2;m(\varphi)). \tag{16}$$

Also, $\xi(T)$ and $m(T)$ are obtained by solving Eq. (12) together with Eq. (15). In this case, the following relation holds: $dV(\varphi^2;m(\varphi))/d\varphi|_{\varphi=\xi}=\partial V(\varphi^2;m(\varphi))/\partial\varphi|_{\varphi=\xi}$.

To improve particle properties at finite T, it is more efficient to apply PMS or FAC conditions directly to the two-point functions [27]. In Ref. [14], FAC with $L=n=2$ was used for the boson self-energy calculated up to two loops. We will adopt a similar condition in Sec. III when we analyze spectral functions of the soft modes.

C. UV divergence in the resumed perturbation

We briefly mention here the reason why the renormalization in resumed perturbation is not a trivial issue.

In the naive perturbation theory, there arises no new UV divergences at $T\neq0$ because of the natural cutoff from the Boltzmann distribution function. Therefore, all the UV divergences at finite T are canceled by the counterterms prepared at $T=0$. This statement has been proved in imaginary-time and real-time formalisms [19].

On the other hand, in self-consistent methods at $T \neq 0$, the situation is not so simple since the tree-level propagators have T-dependent mass [such as $m(T)$ in the above] which contains higher loop contributions through the self-consistent gap equation [9].

In fact, in most of the self-consistent methods applied so far (except for Ref. [14]), the renormalization is taken into account ''after'' imposing the gap equation. This procedure not only makes the renormalization nontrivial and hard in higher orders, but also obscures the origin of the UV divergences. On the contrary, in OPT explained in the previous subsection, the renormalization is performed ''before'' imposing the gap equation. In other words, the UV divergences are already removed in step 2, and a ''finite'' gap equation is obtained from the outset in step 3.

D. Renormalization in OPT

We now prove the order-by-order renormalization in OPT. Let us first rewrite Eq. (7) as

$$\mathcal{L}(\phi;\mu^2) = \mathcal{L}(\phi;m^2) + \frac{1}{2}\chi\phi^2 + \left[\frac{1}{2}B\chi\phi^2 + D\chi^2 - 2Dm^2\chi\right]. \tag{17}$$

Since we use the symmetric and mass independent renormalization scheme (such as the $\overline{\text{MS}}$ scheme), any Green's function generated by $\mathcal{L}(\phi;m^2)$ can be renormalized solely by the coefficients A, B, C, and D in $\mathcal{L}(\phi;\mu^2)$.

Suppose we make a multiple insertion of the composite operator $(1/2)\chi\phi^2$ to the Green's function generated by $\mathcal{L}(\phi;m^2)$. The question is whether new divergences induced by the operator insertion are made finite only by the last three counterterms in Eq. (17). (Note that B and D are already fixed in step 1, and we do not have any freedom to change them.)

The above problem is obviously related to the renormalization of composite operators. In fact, the standard method [29] tells us that necessary counterterms to remove the divergences induced by the insertion of $(1/2)\chi\phi^2$ are written as

$$\frac{1}{2}(ZZ_{\phi^2}^{-1} - 1)\chi\phi^2 + \Delta_2\chi^2 + \Delta_1\chi. \tag{18}$$

Here Z_{ϕ^2} is the renormalization constant for the composite operator ϕ^2, and is necessary to remove the divergence in Fig. 2(A). Δ_2 and Δ_1 are necessary to remove the overall divergences in Fig. 2(B) and in Fig. 2(C), respectively.

Now, one can prove that Eq. (18) coincides with the last three terms in Eq. (17):

$$ZZ_{\phi^2}^{-1} - 1 = B, \quad \Delta_2 = D, \quad \text{and} \quad \Delta_1 = -2Dm^2. \tag{19}$$

The first equation is obtained by the definition $B = Z_\mu Z - 1$ and an identity

$$Z_{\phi^2} = Z_\mu^{-1}. \tag{20}$$

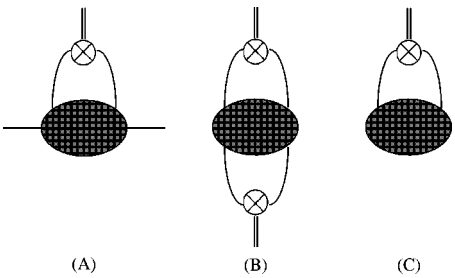

FIG. 2. Diagrams which contain UV divergences as a result of the multiple insertion of $(1/2)\chi\phi^2$. (A) corresponds to a single insertion with two external lines. (B) and (C) have no external lines with a single insertion and a double insertion, respectively.

The overall divergence of the vacuum diagram with no external legs is removed by the c-number counterterm Dm^4 in $\mathcal{L}(\phi;m^2)$. Therefore, the last two equations in Eqs. (19) are obtained as

$$\Delta_1 = -\left(\frac{\partial}{\partial m^2}\right)[Dm^4] = -2Dm^2, \tag{21}$$

$$2\Delta_2 = \left(\frac{\partial}{\partial m^2}\right)^2[Dm^4] = 2D. \tag{22}$$

For completeness, an explicit proof of Eqs. (20), (21), (22) is given in Appendix A.

Equation (19) shows clearly that all the necessary counterterms in OPT are supplied solely by the original Lagrangian $\mathcal{L}(\phi;\mu^2)$. Let us now define $\chi^j\Gamma_R^{(n,j)}(\lambda,m^2)$ as a renormalized n-point proper vertex with insertion of $(1/2)\chi\phi^2$ by j times. (Here the external momentums are not written explicitly.) The counterterms in Eq. (18) together with Eqs. (19) assure the finiteness of $\Gamma_R^{(n,j)}$. Since the proper vertex can be expanded as $\chi^j\Gamma_R^{(n,j)} = \delta^j\Sigma_{l=0}^{\infty}\gamma_l\delta^l$, each coefficient γ_l is also finite. This implies that $\chi^j\Gamma_R^{(n,j)}$ can be made finite order by order in OPT.

Three comments are in order here.

(i) Because the renormalization is already carried out in step 2, one obtains finite gap equations from the beginning in step 3. Our procedure ''resummation after renormalization'' has several advantages over the conventional procedure ''resummation before renormalization'' where UV divergences are hoped to be canceled after imposing the gap equation. The difference between the two is prominent especially in higher order calculations.

(ii) The decomposition (6) should be done both in the mass term and the counterterms. This guarantees the order-by-order renormalization in our modified loop expansion. In Ref. [14], the order-by-order renormalization was checked up to two-loop order in ϕ^4 theory at high T. Our proof shows that this nice feature holds in any higher orders in OPT. On the other hand, if one keeps the original counterterm $(1/2)B\mu^2\phi^2 + D\mu^4$ without the decomposition (6), L-loop diagrams with $L > M$ must be taken into account to remove the UV divergences in the M-loop order (see, e.g., the last reference in [16]). This is an unnecessary complication due to the inappropriate treatment of the counterterms.

(iii) As long as we stay in the low energy region far below the Landau pole, we need not address the issue of the triviality of ϕ^4 theory [28]: Perturbative renormalization in OPT works in the same sense as that in the naive perturbation.

E. Nambu-Goldstone theorem

The procedure and the renormalization in OPT discussed above do not receive modifications even if the Lagrangian has global symmetry. For $O(N)$ ϕ^4 theory, one needs to replace ϕ and ϕ^2 by $\vec{\phi}=(\phi_0,\phi_1,\ldots,\phi_{N-1})$ and $\vec{\phi}^2$, respectively, in all the previous formulas. In the symmetry-broken phase of such theory, the NG theorem and massless NG bosons are guaranteed in each order of the modified loop expansion in OPT for arbitrary N. To show this, it is most convenient to start with the thermal effective potential $V(\vec{\varphi}^2)$. By the definition of the effective potential, $V(\vec{\varphi}^2)$ has manifest $O(N)$ invariance if it is calculated in all orders.

In OPT, V calculated up to Lth loops $V_L(\vec{\varphi}^2;m)$ has also manifest $O(N)$ invariance, because our decomposition (6) used in Eq. (7) does not break $O(N)$ invariance. Once V_L has invariance under the $O(N)$ rotation ($\varphi_i\to\varphi_i+i\theta^a T^a_{ij}\varphi_j$), the immediate consequence is the standard identity

$$\frac{\partial V_L(\vec{\varphi}^2;m)}{\partial\varphi_j}T^a_{ji}=-\frac{\partial^2 V_L(\vec{\varphi}^2;m)}{\partial\varphi_i\partial\varphi_j}T^a_{jk}\varphi_k, \tag{23}$$

with $\mathbf{T}^a$ being the generator of the $O(N)$ symmetry. Equation (23) is valid for arbitrary L, m, and N.

At the stationary point where the left-hand side (LHS) of Eq. (23) vanishes, there arises massless NG bosons for $T^a_{jk}\varphi_k\neq 0$, since the RHS of Eq. (23) is equal to $-\mathcal{D}^{-1}_{ij}(0)T^a_{jk}\phi_k$ where $\mathcal{D}_{ij}(0)$ is the Matsubara propagator at zero frequency and momentum calculated up to Lth loops. Thus the existence of the NG bosons is proved independent of the structure of the gap equation in step 3.

It is instructive here to show some unjustified approximations which lead to the breakdown of the NG theorem. Many of the self-consistent methods applied so far suffer from these problems [30].

(i) Suppose one takes into account only a part of the diagrams for a given number of loops. Then the pion is no longer massless even if the symmetry is spontaneously broken. Although this is a trivial point, sometimes such an approximation is adopted in the literature: taking only the self-energy from the four-point vertex and neglecting that from the three-point vertex is a typical example.

(ii) Introducing m^2 in the $O(N)$-symmetric way as Eq. (6) is a key for the NG theorem to hold in each order of the loop expansion in OPT. Suppose that we make a general decomposition such as

$$\mu^2\delta_{ij}=m^2_{ij}-(m^2_{ij}-\mu^2\delta_{ij}), \tag{24}$$

with $m^2_{ij}\neq m^2\delta_{ij}$. This leads to an $O(N)$ noninvariant effective potential, and the relation (23) is not guaranteed in any finite order of the loop expansion. For example, when the $O(N)$ symmetry is spontaneously broken down to $O(N-1)$, one may be tempted to make a decomposition $m^2_{ij}=m^2_0$ $(i=j=0)$, $m^2_{ij}=m^2_1$ $(i=j\neq 0)$, and $m^2_{ij}=0$ $(i\neq j)$. This leads to an effective potential $V_L(\varphi_0^2,\Sigma_{i=1}^{N-1}\varphi_i^2;m_0,m_1)$ which has only $O(N-1)$ invariance. It implies that Eq. (23) holds only for generators which do not mix φ_0 with $\varphi_{i\neq 0}$. However, Eq. (23) for those generators alone is not enough to prove the existence of NG bosons: In fact, $\varphi_{k\neq 0}$ on the RHS of Eq. (23) vanishes in the $O(N-1)$-symmetric ground state, and no constraints are obtained for $\mathcal{D}^{-1}_{ij}(0)$.

III. APPLICATION TO THE $O(4)$ σ MODEL

Let us apply OPT to study the soft mode associated with chiral transitions. Our main goal is to investigate the spectral functions of the soft modes at finite T:

$$\rho_\phi(\omega,\mathbf{k};T)=-\frac{1}{\pi}\mathrm{Im}\,D^R_\phi(\omega,\mathbf{k};T). \tag{25}$$

Here D^R_ϕ is the retarded correlation function

$$D^R_\phi(\omega,\mathbf{k};T)=-i\int d^4x e^{ikx}\theta(t)\langle[\phi(t,\mathbf{x}),\phi(0,\mathbf{0})]\rangle, \tag{26}$$

where $\langle\cdot\rangle$ denotes thermal expectation value, and $\phi(t,\mathbf{x})$ is $\bar{q}q(t,\mathbf{x})$ or $\bar{q}i\gamma_5\vec{\tau}q(t,\mathbf{x})$ in QCD.

This spectral function was first studied using the Nambu–Jona-Lasinio model of QCD in the large N_c limit [31]. The analysis shows that the scalar meson σ, which has a large width due to the strong decay $\sigma\to 2\pi$, decreases its mass as T increases. Eventually, σ shows up as a sharp resonance near the critical point of the chiral transition. The detectability of such a resonance was studied in the context of ultrarelativistic heavy-ion collisions [32]. Also, the spectral integrals in QCD at finite T were studied using the operator product expansion [33].

In the following, we will adopt a toy model [$O(4)$ linear σ model] to study the effect of mode couplings (interaction among the soft modes) in the one-loop level at finite T. This model shares a common symmetry and dynamics with QCD and has been used to study real-time dynamics and critical phenomena [34,35].

A. Determination of the parameters at $T=0$

The $O(4)$ σ model reads

$$\mathcal{L}=\frac{1}{2}[(\partial\vec{\phi})^2-\mu^2\vec{\phi}^2]-\frac{\lambda}{4!}(\vec{\phi}^2)^2+h\sigma + \frac{1}{2}A(\partial\vec{\phi})^2-\frac{1}{2}B\mu^2\vec{\phi}^2-\frac{\lambda}{4!}C(\vec{\phi}^2)^2+D\mu^4, \tag{27}$$

with $\vec{\phi}=(\sigma,\vec{\pi})$. $h\sigma$ is an explicit chiral-symmetry-breaking term [36]. A, B, C, and D in one-loop order are

$$A=0,\quad B=\frac{\lambda}{16\pi^2}\frac{1}{\varepsilon},\quad C=\frac{\lambda}{8\pi^2}\frac{1}{\varepsilon},\quad D=-\frac{1}{16\pi^2}\frac{1}{\varepsilon}, \tag{28}$$

TABLE I. Vacuum parameters corresponding to $m_\sigma^{peak}=550,\ 750,\ 1000$ MeV.

m_σ^{peak} (Mev)	μ^2 (MeV^2)	λ	h (MeV^3)	κ (MeV)	Γ (MeV)
550	-284^2	73.0	123^3	255	260
750	-375^2	122	124^3	325	657
1000	-469^2	194	125^3	401	995

where $1/\bar{\varepsilon}\equiv 2/(4-n)-\gamma+\log(4\pi)$, with γ being the Euler constant.

When SSB takes place ($\mu^2<0$), the replacement $\sigma\to\sigma+\xi$ in Eq. (27) leads to the tree-level masses of σ and π:

$$m_{0\sigma}^2=\mu^2+\frac{\lambda}{2}\xi^2,\quad m_{0\pi}^2=\mu^2+\frac{\lambda}{6}\xi^2. \tag{29}$$

The expectation value ξ at $T=0$ is determined by the stationary condition for the standard effective potential $\partial V(\vec{\varphi})/\partial\varphi_j=0$.

Later we will take a special FAC condition in which m^2 deviates from μ^2 only at $T\neq 0$, so that the naive loop expansion at $T=0$ is valid. The renormalized couplings μ^2, λ, and h can thus be determined by the following physical conditions in the naive loop expansion at zero T.

(i) The on-shell condition for the pion, $D_\pi^{-1}(k^2=m_\pi^2)=0$, where $m_\pi=140$ MeV, and D_π is the causal propagator for the pion in one-loop order.

(ii) Partially conserved axial-vector current (PCAC) relation in one loop: $f_\pi m_\pi^2=h\sqrt{Z_\pi}$. Here $f_\pi=93$ MeV, and Z_π is the *finite* wave function renormalization constant for the pion on its mass shell.

(iii) The peak position of the spectral function in the σ channel ($\equiv m_\sigma^{peak}$) is taken to be 550 MeV, 750 MeV, or 1000 MeV.

$m_\sigma^{peak}=550$ MeV in (iii) is consistent with recent reanalyses of the π-π scattering phase shift [37]. However, our main conclusions do not suffer a qualitative change by other choices, 750 MeV and 1000 MeV. Instead of m_σ^{peak}, one may take the π-π scattering phase shift itself as a condition to determine parameters [34]. However, for the discussions in the following, such sophistication is not necessary.

We still have the freedom to choose the renormalization point κ. Instead of trying to determine optimal κ by the renormalization group equation for the effective potential [38], we take a simple and physical condition $m_{0\pi}=m_\pi=140$ MeV which is suitable for our later purpose. This choice has two advantages: (a) The one-loop pion self-energy $\Sigma_\pi(k^2)$ vanishes at the tree mass, $\Sigma_\pi(k^2=m_{0\pi}^2)=\Sigma_\pi(k^2=m_\pi^2)=0$, where we have used condition (i) together with $m_{0\pi}=m_\pi$. (b) The spectral function in the σ channel starts from a correct continuum threshold in the one-loop level. [In the loop expansion, $\rho_\sigma(\omega,\mathbf{0})$ has a physical threshold at $\omega=2m_\pi=280$ MeV only if $m_{0\pi}=m_\pi$.]

The resultant parameters are summarized in Table I. The spectral functions ρ_σ and ρ_π defined in Eq. (25) at $T=0$ with $s\equiv\omega^2-\mathbf{k}^2$ are shown in Fig. 3. In the π channel, there are one particle pole and a continuum starting from the threshold $\sqrt{s_{th}}=m_{0\pi}+m_{0\sigma}$. $\sqrt{s_{th}}$ is the point where the channel $\pi+\sigma$ opens. In the σ channel, the spectral function starts from the threshold $2m_{0\pi}=280$ MeV and shows a broad peak centered around $\sqrt{s}=m_\sigma^{peak}$. The half width of the peak is 260 MeV, 657 MeV, and 995 MeV for $m_\sigma^{peak}=550$ MeV, 750 MeV, and 1000 MeV, respectively. The large width of σ is due to a strong σ-2π coupling in the linear σ model. The corresponding σ pole is located far from the real axis on the complex s plane.

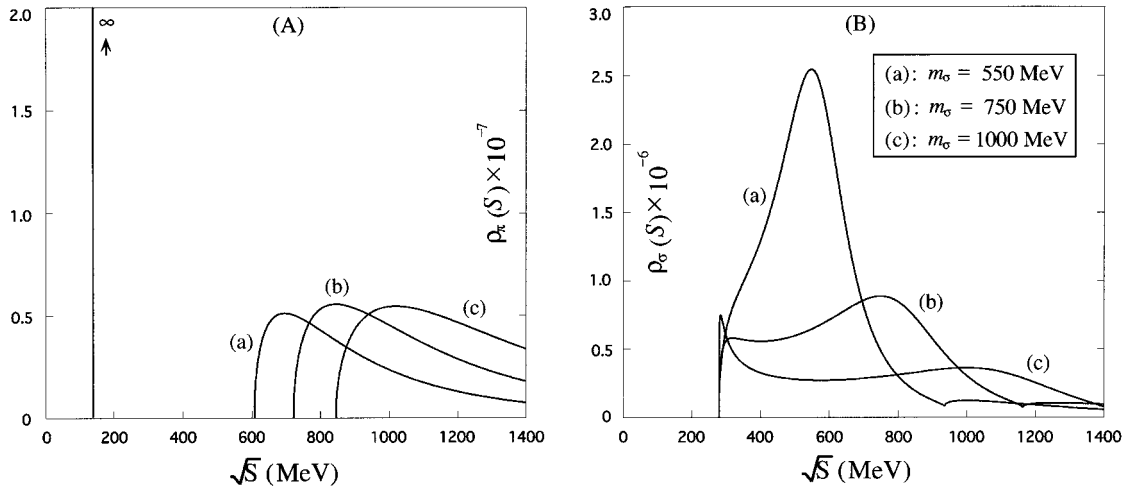

FIG. 3. Spectral functions at $T=0$ in the π channel (A) and in the σ channel (B) for $m_\sigma^{peak}=550$ MeV, 750 MeV, and 1000 MeV.

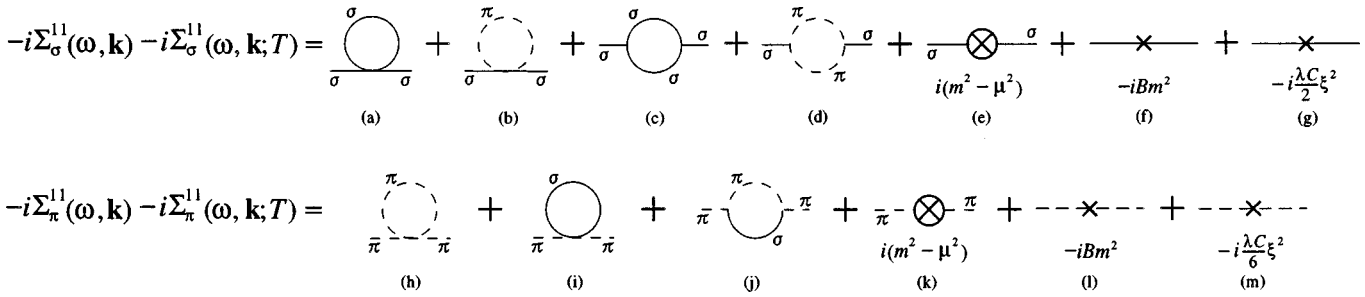

FIG. 4. One-loop self-energy Σ^{11} for σ and π in the modified loop expansion at finite T.

B. Application of OPT

Now let us proceed to step 2 in OPT and rewrite Eq. (27) as

$$\mathcal{L}=\frac{1}{2}[(\partial\vec{\phi})^2-m^2\vec{\phi}^2]-\frac{\lambda}{4!}(\vec{\phi}^2)^2+\frac{1}{2}\chi\vec{\phi}^2+h\sigma - \frac{1}{2}Bm^2\vec{\phi}^2-\frac{\lambda}{4!}C(\vec{\phi}^2)^2+Dm^4. \tag{30}$$

Since $\chi(=m^2-\mu^2)$ is already a one-loop order, we have neglected the terms proportional to $B\chi$, $D\chi^2$, and $D\chi$ which are two-loop or higher order.

When SSB takes place ($\sigma\to\sigma+\xi$), the tree-level masses to be used in the modified loop expansion read

$$m^2_{0\sigma}=m^2+\frac{\lambda}{2}\xi^2, \quad m^2_{0\pi}=m^2+\frac{\lambda}{6}\xi^2. \tag{31}$$

Since m^2 will eventually be a function of T, the tree masses running in the loops are not necessary tachyonic at finite T contrary to the naive loop expansion (see the discussion in Sec. II A).

The thermal effective potential $V(\vec{\varphi};m)$ is calculated in the standard manner except for the extra terms proportional to χ. The Gibbs free energy $G(\xi;m)\equiv V(\vec{\varphi}=(\xi,\mathbf{0});m)$ in the one-loop level reads

$$G(\xi;m)=\frac{1}{2}\mu^2\xi^2+\frac{\lambda}{4!}\xi^4-h\xi + \frac{1}{64\pi^2}\left[m^4_{0\sigma}\ln\left|\frac{m^2_{0\sigma}}{\kappa^2e^{3/2}}\right|+3m^4_{0\pi}\ln\left|\frac{m^2_{0\pi}}{\kappa^2e^{3/2}}\right|\right] + T\int\frac{d^3k}{(2\pi)^3}[\ln(1-e^{-E_\sigma/T})+3\ln(1-e^{-E_\pi/T})], \tag{32}$$

where $E_\phi\equiv\sqrt{\mathbf{k}^2+m^2_{0\phi}}$. Although this has a similar structure to the standard free energy in the naive loop expansion, the coefficient of the first term in the RHS of Eq. (32) is μ^2 instead of m^2. This is because we have an extra mass term proportional to χ in the one-loop level. The stationary point ξ is obtained by

$$\frac{\partial V(\vec{\varphi};m)}{\partial\varphi_i}\Big|_{\vec{\varphi}=(\xi,\mathbf{0})}=\frac{\partial G(\xi;m)}{\partial\xi}=0. \tag{33}$$

Since the derivative with respect to ξ does not act on m, this gives a solution ξ as a function of T and m. By imposing another condition on m (step 3), one eventually determines both ξ and m for given T.

At finite T, the retarded propagator has the general form

$$iD^R_\phi(\omega,\mathbf{k};T)=\frac{i}{k^2-m^2_{0\phi}-\Sigma^R_\phi(\omega,\mathbf{k};T)}, \tag{34}$$

with $k^2=\omega^2-\mathbf{k}^2$. The spectral function is then written as

$$\rho_\phi(\omega,\mathbf{k};T)=-\frac{1}{\pi}\frac{\mathrm{Im}\,\Sigma^R_\phi}{(k^2-m^2_{0\phi}-\mathrm{Re}\,\Sigma^R_\phi)^2+(\mathrm{Im}\,\Sigma^R_\phi)^2}. \tag{35}$$

The retarded self-energy Σ^R_ϕ is related to the 11-component of the 2×2 self-energy in the real-time formalism [39]:

$$\mathrm{Re}\,\Sigma^R_\phi(\omega,\mathbf{k};T)=\mathrm{Re}\,\{\Sigma^{11}_\phi(\omega,\mathbf{k})+\Sigma^{11}_\phi(\omega,\mathbf{k};T)\}$$

$$\mathrm{Im}\,\Sigma^R_\phi(\omega,\mathbf{k};T)=\tanh\left(\frac{\omega}{2T}\right)\mathrm{Im}\{\Sigma^{11}_\phi(\omega,\mathbf{k}) + \Sigma^{11}_\phi(\omega,\mathbf{k};T)\}. \tag{36}$$

Here $\Sigma^{11}_\phi(\omega,\mathbf{k};T)$ is defined as a part with an explicit T dependence through the Bose-Einstein distribution, while $\Sigma^{11}_\phi(\omega,\mathbf{k})$ is the part which has only an implicit T dependence through $m(T)$ and $\xi(T)$. In the one-loop level, Σ^{11}_ϕ can be calculated only by the 11-component of the free propagator:

$$iD^{11}_{0\phi}(k^2;T)=\frac{i}{k^2-m^2_{0\phi}+i\epsilon}+2\pi n_B\delta(k^2-m^2_{0\phi}), \tag{37}$$

with $n_B=[e^{\omega/T}-1]^{-1}$.

One-loop diagrams in OPT for Σ^{11}_ϕ are shown in Fig. 4. Their explicit forms are given in Appendix B. The NG theorem discussed in Sec. II E can be explicitly checked by comparing Eq. (33) and the inverse pion propagator at zero momentum, $[D^R_\pi(0,\mathbf{0};T)]^{-1}$.

C. Cancellation of T-dependent infinities

It is instructive here to show explicitly how the UV divergences discussed in Sec. II D are canceled in one-loop order. The divergent part of $\Sigma_\pi^R(\omega,\mathbf{k};T)$ from the diagrams of Figs. 4(h), 4(i), 4(j) reads

$$\begin{aligned}\Sigma_\pi^R[(h)+(i)+(j)] &\to -\frac{\lambda}{16\pi^2\bar{\varepsilon}} \\ &\quad\times\left(\frac{5}{6}m_{0\pi}^2(T)+\frac{1}{6}m_{0\sigma}^2(T)+\frac{\lambda\xi^2(T)}{9}\right) \\ &= -\frac{\lambda}{16\pi^2\bar{\varepsilon}}\left(m^2(T)+\frac{1}{3}\lambda\xi^2(T)\right) \\ &= -\Sigma_\pi^R[(l)+(m)], \end{aligned} \tag{38}$$

where Eq. (31) has been used. Namely, the terms proportional to $m^2(T)$ in Figs. 4(h), 4(i) are canceled by the counterterm proportional to Bm^2, while the terms proportional to $\xi^2(T)$ in Figs. 4(h), 4(i), 4(j) are canceled by the usual counterterms proportional to C. In this way, the T-dependent divergences proportional to $m^2(T)$ newly appearing in OPT are automatically canceled by the T-dependent counterterms obtained by the shift $\mu^2=m^2-\chi$. The divergence of the free energy proportional to m^4 is also canceled by the last counterterm in Eq. (17).

Note that the divergences proportional to χ start to appear from the two-loop level. They are removed by the counterterms proportional to χ obtained by the shift $\mu^2=m^2-\chi$.

D. FAC condition for m^2

Since we are interested in the spectral functions in the one-loop level, a best way to determine m^2 is to use the two-point function in the π channel. In [14], a FAC condition (14) for the two-loop self-energy at zero momentum $(L=n=2)$ was taken to obtain a gap equation for ϕ^4 theory above T_c.

The corresponding condition in our model with $L=n=1$ reads

$$\Sigma_\pi^R(\omega=0,\mathbf{0};T)=\Sigma_\pi^{11}(\omega=0,\mathbf{0})+\Sigma_\pi^{11}(\omega=0,\mathbf{0};T)=0. \tag{39}$$

This is a condition that the one-loop correction to the self-energy must be as small as possible in the resumed perturbation theory. [Note that Im $\Sigma_\pi^R(\omega=0,\mathbf{0};T)$ vanishes identically.] Unfortunately, Eq. (39) is incompatible with the condition which we adopted at $T=0$ in Sec. III A to find an optimal renormalization point κ:

$$\Sigma_\pi^R(\omega=m_{0\pi},\mathbf{0};T=0)=0. \tag{40}$$

A hybrid condition which does not destroy Eq. (40) and simultaneously leads to a valid gap equation is

$$\Sigma_\pi^{11}(\omega=m_{0\pi},\mathbf{0})+\Sigma_\pi^{11}(\omega=0,\mathbf{0};T)=0. \tag{41}$$

The explicit form of this FAC condition can be read from Eq. (B2) in Appendix B:

$$\begin{aligned} m^2=\mu^2&+\frac{\lambda}{6}\left[5\tilde{I}_\pi^{(1)}+\tilde{I}_\sigma^{(1)}-i\frac{2}{3}\lambda\xi^2\tilde{I}^{(3)}\right]_{\omega=m_{0\pi}} \\ &+\frac{\lambda}{6}\left[5F_\pi^{(1)}+F_\sigma^{(1)}-i\frac{2}{3}\lambda\xi^2(F^{(4)}+F^{(5)})\right]_{\omega=0}. \end{aligned} \tag{42}$$

The first (second) line is from the first (second) term on the LHS of Eq. (41). The functions I and F are given in Appendix B ($\tilde{I}$ is defined as the finite part of I).

At $T=0$, the second term on the LHS of Eq. (41), $\Sigma_\pi^{11}(\omega,\mathbf{k};T=0)$, vanishes by definition, and Eq. (41) formally reduces to Eq. (40). However, we calculate Eq. (40) in the naive loop expansion without introducing m^2 as discussed in Sec. III A, while Eq. (41) is calculated with m^2 even at $T=0$. Therefore, they are consistent only when

$$m^2(T=0)=\mu^2. \tag{43}$$

In other words, OPT with the FAC condition (41) applied at $T=0$ is equivalent to the naive loop expansion.

In the symmetric phase at high T where $\xi(T)\simeq 0$, Eq. (42) reduces to

$$m^2=\mu^2+\lambda\left[\int\frac{d^3k}{(2\pi)^3}\frac{n_B(E(m))}{E(m)}+\frac{m^2}{16\pi^2}\ln\frac{m^2}{e\kappa^2}\right], \tag{44}$$

with $E(m)=\sqrt{m^2+\mathbf{k}^2}$. If $T^2\gg m^2$, the first term on the RHS of Eq. (44) dominates and the following solution is obtained:

$$m^2(T)=\mu^2+\frac{\lambda}{12}T^2, \tag{45}$$

which implies that the Debye screening mass at high T can be properly taken into account. Also, both Eqs. (41) and (39) have the same solution (45) for $T^2\gg m^2$ and are consistent with each other. For realistic values of λ in Table I, the condition $T^2\gg m^2$ is not well satisfied and one needs to solve Eq. (41) numerically which will be shown in Sec. III E.

For intermediate values of T, Eq. (41) can effectively sum not only the contributions from the diagrams in Figs. 4(a), 4(b), 4(h), 4(i), but also from those in Figs. 4(c), 4(d), 4(j). Thus, OPT can go beyond the cactus approximation which sums only Fig. 4(a), 4(b), 4(h), 4(i).

Three remarks are in order here.

(i) For sufficiently high T with fixed κ, Eq. (44) ceases to have a solution. In fact, the RHS of Eq. (44) is always larger than the LHS above a limiting temperature $T_l=500,430,420$ MeV for $m_\sigma^{peak}(T=0)=500,750,1000$ MeV, respectively. This indicates that our one-loop analysis in OPT is not sufficient for $T>T_l$. One may try a renormalization group improvement by choosing, e.g., $\kappa=T$ to cure this problem. However, since λ in Table I is rather large, one encounters the Landau pole in the running coupling $\lambda(T)$ located at $T=440,450,490$ MeV for $m_\sigma^{peak}(T=0)$

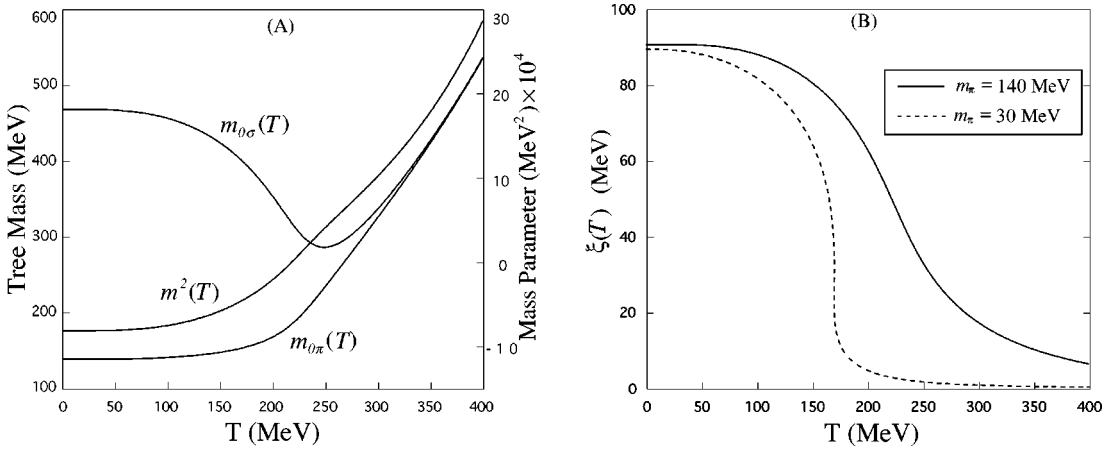

FIG. 5. (A) Masses in the tree level $m_{0\pi}(T)$ and $m_{0\sigma}(T)$, shown with left vertical scale, and the mass parameter $m^2(T)$ with the right vertical scale. (B) $\xi(T)$ for $m_\pi(T=0)=140$ MeV and 30 MeV with $m_\sigma^{peak}(T=0)=550$ MeV.

$=500,750,1000$ MeV, respectively. This again sets an upper bound of T beyond which the one-loop analysis in OPT is not reliable.

(ii) To study the possible variations of the FAC condition, Eq. (41), we have examined the following three cases. (a) Taking the high T formula, Eq. (45), in place of Eq. (41). (b) Replacing the second term on the LHS of Eq. (41) by $C_1 \equiv \Sigma_\pi^{11}(\omega=m_{0\pi},\mathbf{0};T)$. (c) Replacing the second term on the LHS of Eq. (41) by $C_2 \equiv \mathrm{Re}\,\Sigma_\pi^{11}(\omega=m_{0\pi},\mathbf{0};T)$. In case (a), because of the lack of self-consistency at low T, $m_{0\pi}(T)$ deviates substantially from $m_\pi(T)$. This leads to an incorrect threshold for the spectral function in the σ channel. In case (b), a real solution for m^2 is not guaranteed, because C_1 is a complex function due to the Landau damping. In case (c), a discontinuity of m^2 at certain T appears, because C_2 has a cusp structure as a function of ω as shown in Fig. 8(C), below. (We will discuss this cusp in Sec. III G.) Therefore, within the FAC condition for the one-loop self-energy, Eq. (41) is almost a unique choice in the sense that it gives a smooth and physically acceptable solution for m^2.

(iii) In place of the FAC condition, one may take the PMS condition. However, to get a sensible gap equation from the PMS condition for the thermal effective potential V, one needs to calculate V at least up to two loops [13]. Unlike the optimized expansion considered in the first reference in [13], we have both Hartree and Fock diagrams in the two-loop order. This complicates the PMS analyses which will be reported elsewhere.

E. Behavior of $m(T)$, $m_{0\phi}(T)$, and $\xi(T)$

In Fig. 5(A) the tree-level masses in Eq. (31) and $m^2(T)$ are shown for $m_\sigma^{peak}(T=0)=550$ MeV. $m_{0\phi}^2(T)$ is not tachyonic and approaches $m^2(T)$ in the symmetric phase. This confirms that our resummation procedure cures the tachyon problem in Sec. II A.

The solid line in Fig. 5(B) shows the chiral condensate $\xi(T)$ obtained by minimizing the free energy for the case $m_\pi(T=0)=140$ MeV, with $m_\sigma^{peak}(T=0)=550$ MeV. $\xi(T)$ decreases uniformly as T increases, which is a typical behavior of the chiral order parameter at finite T away from the chiral limit. As we approach the chiral limit ($h\to 0$ or equivalently $m_\pi\to 0$), $\xi(T)$ develops multiple solutions for a given T, which could be an indication of a first order transition. This will be discussed in more detail in the next subsection. The critical value of the quark mass $m_q^{\rm crit}$ below which the multiple solutions arise is

$$m_q^{\rm crit}/m_q^{\rm phys}=(m_\pi^{\rm crit}/m_\pi^{\rm phys})^2=0.08, \tag{46}$$

where we have used Gell-Mann–Oakes–Renner relation [40] to relate the pion mass with the quark mass. $m_q^{\rm phys}$ is the physical light-quark mass corresponding to $m_\pi^{\rm phys}=140$ MeV. The critical temperature for $m_q^{\rm crit}/m_q^{\rm phys}=0.08$ is $T_c\simeq 170$ MeV. The behavior of $\xi(T)$ for $m_\pi(T=0)=30$ MeV (just below the critical value $m_\pi^{\rm crit}$) is also shown by the dashed line in Fig. 5(B) for comparison.

Figure 6(A) shows $m_{0\phi}^2(T)$ for $m_\sigma^{peak}(T=0)=750,1000$ MeV. The qualitative behaviors are similar to Fig. 5(A). The chiral condensate $\xi(T)$ for $m_\sigma(T=0)=750,1000$ MeV is also shown in Fig. 6(B). $\xi(T)$ is rather insensitive to the change of m_σ^{peak} as far as $m_\pi(T=0)=140$ MeV is imposed.

F. Chiral limit ($h=0$)

In the chiral limit, the FAC condition and the resultant gap equation are drastically simplified and some analytical study becomes possible. Let us carry out this analysis to reveal the nature of the chiral transition near the chiral limit.

For $h=0$, the NG theorem is satisfied for a given m^2 as shown in Sec. II E. Therefore, as far as $\xi\neq 0$ (the NG phase), the total self-energy of the pion must vanish at $(\omega,\mathbf{p})=(0,\mathbf{0})$:

$$m_{0\pi}^2+\Sigma_\pi^R(0,\mathbf{0};T)=0. \tag{47}$$

A simultaneous solution of Eq. (47) and the FAC condition (41) is $m_{0\pi}^2=\Sigma_\pi^R(0,\mathbf{0};T)=0$, which leads to

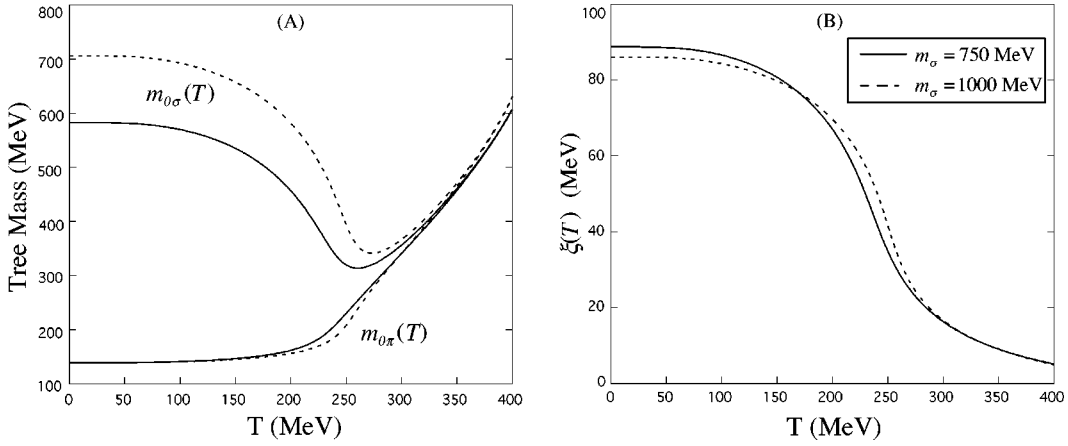

FIG. 6. (A) Masses in the tree level, $m_{0\pi}(T)$ and $m_{0\sigma}(T)$. (B) $\xi(T)$ for $m_\sigma^{peak}(T=0)=750$ MeV and 1000 MeV with $m_\pi=140$ MeV.

$$m^2=-\frac{\lambda}{6}\xi^2, \quad m_{0\pi}^2=0, \quad \text{and} \quad m_{0\sigma}^2=\frac{\lambda}{3}\xi^2. \tag{48}$$

The stationary condition (33) always has a solution $\xi=0$ for $h=0$ (the Wigner phase). The gap equation to determine the other solutions in the NG phase is obtained by substituting Eq. (48) into Eq. (33):

$$0=\mu^2+\frac{\lambda}{6}\xi^2+\frac{\lambda^2}{96\pi^2}\xi^2\ln\left|\frac{\lambda\xi^2}{3\kappa^2 e}\right| + \frac{\lambda}{2}\int\frac{d^3k}{(2\pi)^3}\left(\frac{n_B(E_\sigma)}{E_\sigma}+\frac{n_B(E_\pi)}{E_\pi}\right), \tag{49}$$

where $E_\sigma=\sqrt{\mathbf{k}^2+\lambda\xi^2/3}$ and $E_\pi=|\mathbf{k}|$.

The numerical solution of Eq. (49) is given by the solid line in Fig. 7. As can be seen from the figure, there are two nonvanishing solutions for ξ in the range $T_1=126$ MeV $<T<T_2=153$ MeV, which is a typical behavior of the first order phase transition. For comparison, the case slightly away from the chiral limit is shown by the dashed lines in Fig. 7.

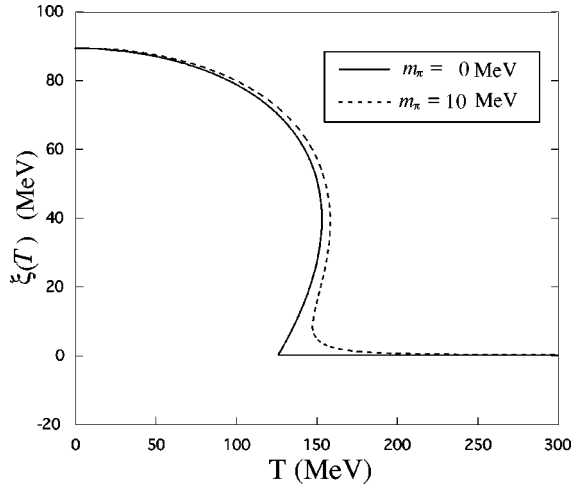

FIG. 7. $\xi(T)$ for $m_\sigma^{peak}(T=0)=550$ MeV with $m_\pi=0$ MeV and $m_\pi=10$ MeV.

T_1 and the behavior of $\xi(T)$ for $T\sim T_1$ can be solved analytically by expanding Eq. (49) in terms of ξ near $\xi=0$: Only the first term μ^2 and the last two terms proportional to the Bose-Einstein distribution are relevant, and one obtains

$$T_1=\sqrt{\frac{12}{\lambda}}|\mu|, \quad \xi(T>T_1)\simeq\frac{4\pi}{\sqrt{3\lambda}}(T-T_1). \tag{50}$$

The existence of multiple solutions of the gap equation for the $O(4)$ σ model in the mean-field approach has been known for a long time [41]. Our analyses above confirm this feature within the framework of OPT. However, as is discussed in the second reference of [41], this first order nature is likely to be an artifact of the mean-field approach, since the higher loops of massless π and almost massless σ are not negligible near T_1, and they could easily change the order of the transition [42]. In fact, renormalization group analyses as well as direct numerical simulation on the lattice indicate that the $O(4)$ σ model has a second order phase transition [43].

In the following, we will go back to the the real world with $m_\pi(T=0)=140$ MeV, where the gap equation has only one solution for a given T.

G. Spectral function at $T\neq 0$

In Figs. 8(A), 8(B), we show the spectral functions $\rho_{\pi,\sigma}(\omega,\mathbf{0};T)$ for $T=50,120,145$ MeV with $m_\sigma^{peak}(T=0)=550$ MeV.

In the π channel, a continuum develops for $0<\omega<m_{0\sigma}-m_{0\pi}$. This originates from the induced ''decay'' by the scattering with thermal pions in the heat bath: $\pi+\pi^{\text{thermal}}\rightarrow\sigma$. Because of this process, the pion acquires a width ~ 50 MeV at $T=145$ MeV, while the peak position does not show appreciable modification. They are in accordance with the Nambu-Goldstone nature of the pion, and are con-

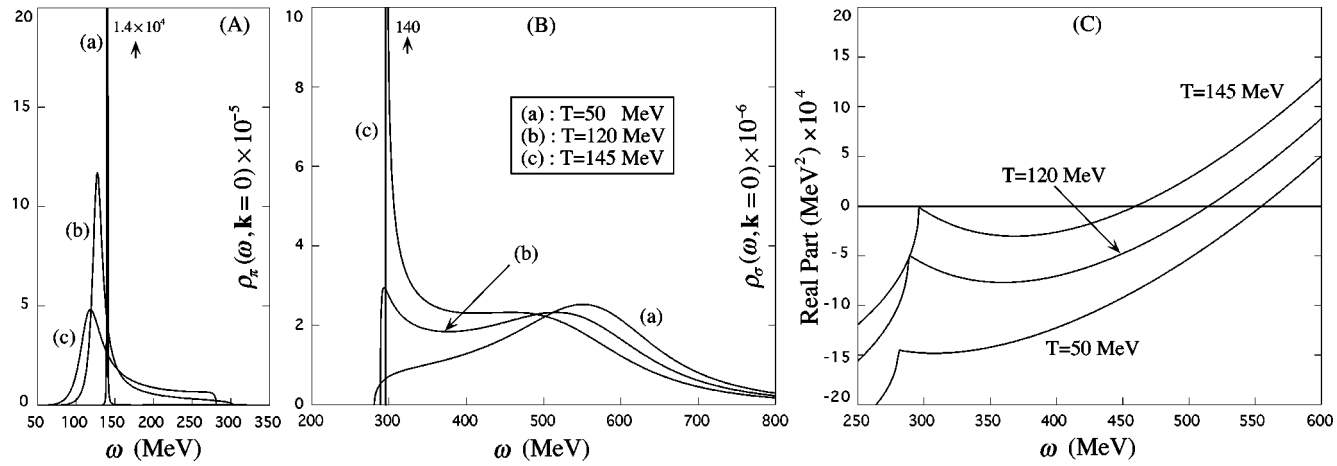

FIG. 8. Spectral function in the π channel (A) and in the σ channel (B) for $T=50,120,145$ MeV with $m_\sigma^{peak}(T=0)=550$ MeV. The real part of $[D_\sigma^R(\omega,0;T)]^{-1}$ as a function of ω is shown in (C).

sistent with other calculations based on the low T expansion [44].

In the σ channel for $0<T<145$ MeV, there are two noticeable modification of the spectral function. One is the shift of the σ peak toward the low mass region. The other is the sharpening of the spectral function just above the continuum threshold starting at $\omega=2m_{0\pi}(T)$.

These features are simply controlled by zeros or approximate zeros of

$$\mathrm{Re}[D_\sigma^R(\omega,\vec{0})]^{-1}=\omega^2-m_{0\phi}^2-\mathrm{Re}\,\Sigma_\sigma^R(\omega,\vec{0};T), \quad (51)$$

which appears in the denominator of the spectral function (35). Note that the imaginary part of $[D_\sigma^R(\omega,\vec{0})]^{-1}$ is a smooth function of ω and does not develop zeros above the threshold. Equation (51) is plotted in Fig. 8(C). For $T<145$ MeV, $\mathrm{Re}[D_\sigma^R(\omega,\vec{0})]^{-1}$ has only one zero for a given T. This zero corresponds to an ''effective'' mass of the σ meson at finite T and roughly corresponds to the position of the broad peak in Fig. 8(B).

On the other hand, as T increases, the cusp in the low ω region starts to create an approximate zero of $\mathrm{Re}[D_\sigma^R(\omega,\vec{0})]^{-1}$. [At $T=145$ MeV, the cusp creates an exact zero as shown in Fig. 8(C).] This is why the peak just above the threshold develops as T increases as shown in Fig. 8(B). The cusp originates from the σ-π-π coupling (the fourth diagram for the sigma self-energy in Fig. 4) and is related to the the continuum threshold by analyticity. The position of the cusp is exactly the point where the continuum starts: $\omega=2m_{0\pi}(T)$.

The approximate shape of the spectral function for $\omega\simeq2m_{0\pi}(T)$ with $T\simeq145$ MeV can be estimated as follows. The first term in the denominator of Eq. (35) approaches zero smoothly as $\omega\to2m_{0\pi}$:

$$[\omega^2-m_{0\phi}^2-\mathrm{Re}\,\Sigma_\sigma^R(\omega,\vec{0})]_{\omega\to2m_{0\pi}}\to0. \quad (52)$$

On the other hand, the imaginary part of the self-energy is a phase space factor multiplied by a smooth and nonzero function f:

$$\mathrm{Im}\,\Sigma_\sigma^R(\omega,\vec{0};T)=\theta(\omega-2m_{0\pi})\sqrt{1-\frac{4m_{0\pi}^2}{\omega^2}}f(\omega,T). \quad (53)$$

Substituting Eqs. (52) and (53) into Eq. (35), one finds

$$\rho_\sigma(\omega\simeq2m_{0\pi},\vec{0};T)=\theta(\omega-2m_{0\pi})\times\frac{1}{\sqrt{1-\frac{4m_{0\pi}^2}{\omega^2}}f(2m_{0\pi},T)}. \quad (54)$$

This explains the enhancement just above the threshold due to the phase space factor.

There is another explanation of the threshold enhancement. Let us start with a sum rule for the spectral function which can be proved by the spectral decomposition of ρ_ϕ:

$$\int_0^\infty\rho_\phi(\omega,\mathbf{k};T)d\omega^2=(A+1)^{-1}, \quad (55)$$

where $Z=A+1$ is the wave function renormalization constant and does not depend on T. Since $A=0$ in one-loop order, the spectral integral is unity for arbitrary T. This fact together with the positivity of ρ_ϕ implies that there is a spectral concentration near the threshold as $m_\sigma^{peak}(T)$ decreases.

Beyond one loop, A is divergent in perturbation theory. However, one can always define a finite and T-independent spectral integral as

$$\int_0^\infty[\rho_\phi(\omega,\mathbf{k};T)-\rho_\phi(\omega,\mathbf{k};T=0)]d\omega^2=0. \quad (56)$$

Therefore, the same argument with the one-loop case holds and a spectral concentration near threshold will occur even beyond one loop. The threshold enhancement in Fig. 8(B), although it occurs at relatively low T, is caused by a combined effect of the partial restoration of chiral symmetry (de-

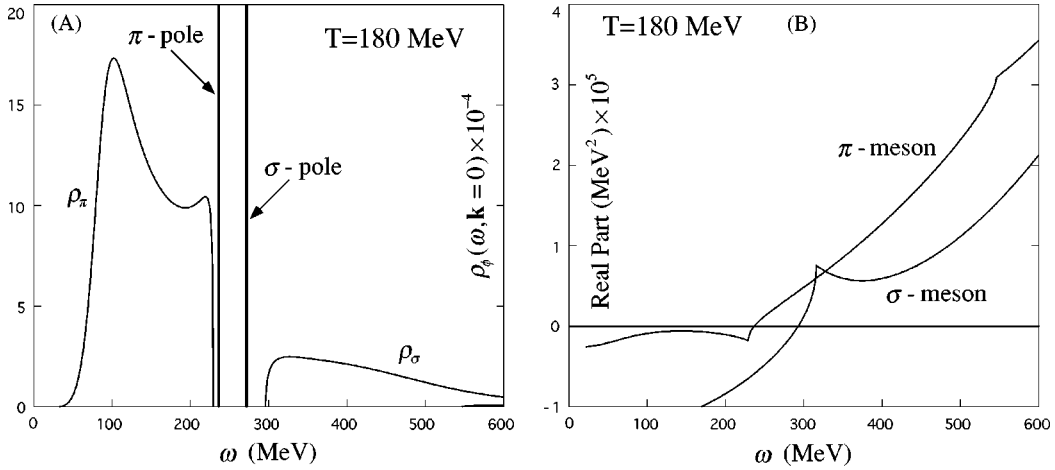

FIG. 9. (A) Spectral functions in the π and σ channels at $T=180$ MeV. (B) The real part of $[D_\pi^R(\omega,0;T)]^{-1}$ and $[D_\sigma^R(\omega,0;T)]^{-1}$ as a function of ω at $T=180$ MeV with $m_\sigma^{peak}(T=0)=550$ MeV.

creasing the ''effective'' mass) and the strong $\sigma-2\pi$ coupling. In the chiral limit, the continuum threshold starts from $\omega=0$, and the enhancement occurs exactly at the critical temperature of chiral transition.

A similar threshold enhancement in the π channel becomes prominent just below $\omega=m_{0\sigma}-m_{0\pi}$ for $T\simeq 165$ MeV. The basic mechanism of this enhancement is the same for the σ case except that $\mathrm{Re}[D_\pi^R(\omega,\vec{0})]^{-1}$ is a deceasing function of T.

The spectral functions of π (σ) at higher temperature exhibits the standard behavior as expected from previous analyses [31,33]. Shown in Fig. 9 are simple σ and π poles and a continuum at $T=180$ MeV. As T increases, these poles gradually merge into a degenerate (chiral symmetric) states. Because of this approximate degeneracy, the normal decay of σ through $\sigma\to 2\pi$ and the induced decay of π through $\pi+\pi\to\sigma$ are kinematically forbidden at high T. This is why the width of σ and π vanishes.

For sufficiently high T, the system is supposed to be in the deconfined phase and the decay $(\sigma,\pi)\to q\bar{q}$ must occur.

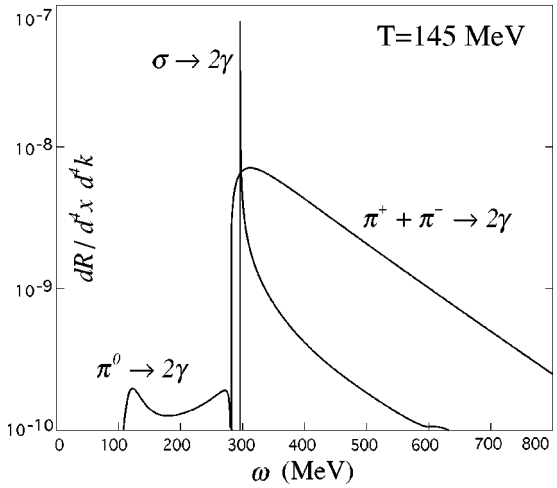

FIG. 10. Diphoton yield per unit space-time volume in the back-to-back kinematics at $T=145$ MeV for $m_\sigma^{peak}(T=0)=550$ MeV.

This is not taken into account in the present linear σ model. A calculation based on the Nambu–Jona-Lasinio model shows, however, that there is still a chance for collective modes to survive as far as T/T_c is not so far from unity [31].

H. Diphoton emission rate through $\sigma\to 2\gamma$

As one of the experimental candidates to see the threshold enhancement in the σ channel, we evaluated the diphoton emission rate from the decay $\sigma\to 2\gamma$ in hot hadronic matter [45]. The diphoton yield (with back-to-back kinematics) per unit space-time volume of a hot hadronic plasma can be written as [46]

$$\frac{dR_\sigma}{d^4x d^4k}=\frac{1}{(2\pi)^4}g_\sigma^2|F_{\sigma\gamma\gamma}(k^2)|^2\omega^4\frac{\rho_\sigma(\omega,\mathbf{k}=0;T)}{e^{\omega/T}-1}, \tag{57}$$

where $k^\mu=(\omega,\mathbf{k})$ denotes the total four-momentum of the diphoton. g_σ is the $\sigma\gamma\gamma$ vertex at zero momentum and $F_{\sigma\gamma\gamma}(k^2)$ is a corresponding form factor. $g_\sigma F_{\sigma\gamma\gamma}$ has a short distant contribution from the constituent-quark loop and a long distant contribution from the pion loop. We took the estimates given in [47] for these contributions. The formula for $\pi^0\to 2\gamma$ is obtained by the replacement $\sigma\to 2\gamma$ in Eq. (57). In this case, g_π is fixed by the axial anomaly, and $F_{\pi\gamma\gamma}$ is taken from an estimate using the chiral quark model [48].

The main background for the above processes is the thermal annihilation of pions: $\pi^+\pi^-\to 2\gamma$. The diphoton yield from $\sigma\to 2\gamma$ and $\pi^0\to 2\gamma$ together with this background at $T=145$ MeV is shown in Fig. 10. The threshold enhancement in the $\sigma\to 2\gamma$ process is significant only in a narrow region of the diphoton invariant mass and in a narrow region of T. A similar conclusion is drawn in another analysis [49].

IV. SUMMARY

In this paper, we have examined optimized perturbation theory (OPT) in detail at finite T. For theories with sponta-

neous symmetry breaking, the loop-wise expansion in OPT is shown to be a suitable scheme to resum higher order terms.

We have shown that OPT naturally cures the two major problems of the naive loop expansion, namely, the breakdown of perturbation series at high $T>T_c$ and the existence of tachyon poles for $T<T_c$.

We have also shown that OPT has several advantages over other resummation methods proposed so far. First of all, the renormalization of the UV divergences, which is not a trivial issue in other methods, can be carried out systematically in the loop expansion in OPT. This is because one can separate the the self-consistent procedure (step 3 in Sec. II B) from the renormalization procedure (step 2 in Sec. II B) in OPT.

Whether the Nambu-Goldstone (NG) theorem is satisfied in resummation methods has been discussed in the literature. We found that the loop expansion in OPT can give a clear view of this problem. The NG theorem is a direct consequence of the invariance of the effective action. Since the OPT presented in this paper does not break the global symmetry of the effective potential in each order of the perturbation, one can prove, without much difficulty, that the NG theorem is satisfied in any give order of the loop expansion in OPT.

In the latter part of this paper, we have applied OPT to the $O(4)$ σ model to study the spectral functions at finite T. The OPT in one-loop order together with a FAC condition for the pion self-energy, we have successfully summed not only the cactus diagrams but also other loop diagrams. We have demonstrated that the spectral function of σ, which does not show a clear resonance at $T=0$, develops a sharp enhancement near the 2π threshold as T approaches T_c. This is due to a combined effect of the partial restoration of chiral symmetry and the strong σ-2π coupling. Although it is rather difficult to observe this enhancement in the diphoton spectrum, further studies will be necessary to reveal the phenomenological implications of this phenomena.

The basic idea of OPT examined in detail in this paper will also have relevance to develop an improved perturbation theory for gauge theories in which the weak-coupling expansion is known to break down in high orders [50]. A generalization of OPT, such as that discussed at step 2 in Sec. II B, will be necessary for this purpose.

ACKNOWLEDGMENTS

The authors would like to thank M. Asakawa, K. Kanaya, T. Kunihiro, T. Matsui, and J. Randrup for useful discussions. This work was partially supported by Grants-in-Aid of the Japanese Ministry of Education, Science and Culture (No. 06102004). S.C. would like to thank the Japan Society of Promotion of Science (JSPS) for financial support.

APPENDIX A: COUNTERTERMS IN OPT

Consider the Lagrangian $\mathcal{L}(\phi;m^2)$ and define $\Gamma_R^{(n,j)}(\lambda,m^2)$ as the the renormalized n-point proper vertex with insertion of the composite operator $\phi^2(x)/2$ by j times. (We do not write the external momenta explicitly.) Applying the counterterms in Eq. (18), $\Gamma_R^{(n,j)}$ is written by the unrenormalized proper vertex $\Gamma_0^{(n,j)}$ and the renormalization constants (Z, Z_{ϕ^2}, Δ_1 and Δ_2) as [29]

$$\Gamma_R^{(n,j)}(\lambda,m^2)=Z^{n/2}Z_{\phi^2}^{-j}\Gamma_0^{(n,j)}(\lambda_0,m_0^2) + (2\Delta_2\delta_{j2}+\Delta_1\delta_{j1})\delta_{n0}, \tag{A1}$$

where the bare quantities with a suffix ''0'' are related to the renormalized quantities as $\lambda_0=Z_\lambda\lambda$, $m_0^2=Z_\mu m^2$ and $\phi_0=\sqrt{Z}\phi$.

To show Eq. (20), consider the proper self-energy $\Gamma_R^{(2,0)}(\lambda,m^2)$ and its derivative with respect to m^2. After a straightforward algebra using Eq. (A1), one finds

$$\frac{\partial}{\partial m^2}\Gamma_R^{(2,0)}(\lambda,m^2)=-ZZ_\mu\Gamma_0^{(2,1)}(\lambda_0,m_0^2) =-Z_\mu Z_{\phi^2}\Gamma_R^{(2,1)}(\lambda,m^2). \tag{A2}$$

Since $\Gamma_R^{(n,j)}$ is finite, Eq. (A2) implies that $Z_\mu Z_{\phi^2}$ must be finite in four dimensions. Now, in the loop expansion with the $\overline{\mathrm{MS}}$ scheme, Z_μ and Z_{ϕ^2} have expansions of the form $1+\Sigma_{l=1}^{\infty}a_l\delta^l$ with a_l containing only the powers of $1/\bar{\varepsilon}$. This fact together with the finiteness of $Z_\mu Z_{\phi^2}$ for $\bar{\varepsilon}\to 0$ immediately leads to Eq. (20), $Z_\mu Z_{\phi^2}=1$.

To show Eq. (21), consider the proper vertex without external legs: $\Gamma_R^{(0,0)}(\lambda,m^2)$. This quantity is a sum of all the one-particle irreducible diagrams + the c-number counterterm Dm^4. Therefore, taking a derivative with respect to m^2 and using Eq. (A1), one finds

$$\frac{\partial}{\partial m^2}\Gamma_R^{(0,0)}(\lambda,m^2)=-ZZ_\mu\frac{1}{V_4}\int_{V_4}d^4x\left\langle\frac{\phi^2(x)}{2}\right\rangle_{1PI}+2Dm^2 =-[\Gamma_R^{(0,1)}(\lambda,m^2)-\Delta_1]+2Dm^2. \tag{A3}$$

Here $\langle\cdot\rangle_{1PI}$ denotes the one-particle irreducible contribution. V_4 denotes the Euclidean four-volume: At $T\neq 0$, $V_4=V_3/T$ with V_3 being the three-volume. Since $\Gamma_R^{(n,j)}$ is finite, Eq. (A3) implies that $2Dm^2+\Delta_1$ must be finite in four dimensions. D and Δ_1 have expansions of the form $\Sigma_{l=1}^{\infty}a_l\delta^l$, with a_l containing only the powers of $1/\bar{\varepsilon}$. Thus one arrives at Eq. (21), $2Dm^2+\Delta_1=0$.

To show Eq. (22), one needs to take the derivative with respect to m^2 one more time:

$$\left(\frac{\partial}{\partial m^2}\right)^2\Gamma_R^{(0,0)}(\lambda,m^2) =Z^2Z_\mu^2\frac{1}{V_4}\int_{V_4}d^4x\int_{V_4}d^4y\left\langle\frac{\phi^2(x)}{2}\frac{\phi^2(y)}{2}\right\rangle_{1PI}+2D =[\Gamma_R^{(0,2)}(\lambda,m^2)-2\Delta_2]+2D. \tag{A4}$$

By a similar argument as above, $D-\Delta_2=0$ follows from Eq. (A4).

APPENDIX B: ONE-LOOP FORMULA FOR THE SELF-ENERGY AT $T \neq 0$

Formulas corresponding to Fig. 4 read

$$-i\Sigma_\sigma^{11}(\omega,\mathbf{k})-i\Sigma_\sigma^{11}(\omega,\mathbf{k};T)=-i\frac{\lambda}{2}[I_\pi^{(1)}+F_\pi^{(1)}+I_\sigma^{(1)}+F_\sigma^{(1)}]+\left(-i\frac{\lambda\xi}{3}\right)^2\frac{3}{2}[I_\pi^{(2)}+2F_\pi^{(2)}+F_\pi^{(3)}]$$
$$+(-i\lambda\xi)^2\frac{1}{2}[I_\sigma^{(2)}+2F_\sigma^{(2)}+F_\sigma^{(3)}]+i(m^2-\mu^2)+\text{counterterms}, \tag{B1}$$

$$-i\Sigma_\pi^{11}(\omega,\mathbf{k})-i\Sigma_\pi^{11}(\omega,\mathbf{k};T)=-i\frac{5\lambda}{6}[I_\pi^{(1)}+F_\pi^{(1)}]-i\frac{\lambda}{6}[I_\sigma^{(1)}+F_\sigma^{(1)}]+\left(-i\frac{\lambda\xi}{3}\right)^2[I^{(3)}+F^{(4)}+F^{(5)}]$$
$$+i(m^2-\mu^2)+\text{counterterms}, \tag{B2}$$

with

$$I_\phi^{(1)}=\kappa^{2\varepsilon}\int\frac{d^4p}{(2\pi)^4}\frac{i}{p^2-m_{0\phi}^2+i\epsilon}, \tag{B3}$$

$$I_\phi^{(2)}=\kappa^{2\varepsilon}\int\frac{d^4p}{(2\pi)^4}\frac{i}{p^2-m_{0\phi}^2+i\varepsilon}\frac{i}{(p+k)^2-m_{0\phi}^2+i\epsilon}, \tag{B4}$$

$$I^{(3)}=\kappa^{2\varepsilon}\int\frac{d^4p}{(2\pi)^4}\frac{i}{p^2-m_{0\sigma}^2+i\varepsilon}\frac{i}{(p+k)^2-m_{0\pi}^2+i\epsilon}, \tag{B5}$$

$$F_\phi^{(1)}=\int\frac{d^4p}{(2\pi)^4}2\pi n_B(|p_0|)\,\delta(p^2-m_{0\phi}^2), \tag{B6}$$

$$F_\phi^{(2)}=i\int\frac{d^4p}{(2\pi)^4}\frac{2\pi n_B(|p_0|)\,\delta(p^2-m_{0\phi}^2)}{(p+k)^2-m_{0\phi}^2+i\epsilon}, \tag{B7}$$

$$F_\phi^{(3)}=\int\frac{d^4p}{(2\pi)^4}(2\pi)^2 n_B(|p_0|)n_B(|p_0+\omega|)\,\delta(p^2-m_{0\phi}^2)\,\delta((p+k)^2-m_{0\phi}^2), \tag{B8}$$

$$F^{(4)}=i\int\frac{d^4p}{(2\pi)^4}\frac{2\pi n_B(|p_0|)\,\delta(p^2-m_{0\sigma}^2)}{(p+k)^2-m_{0\pi}^2+i\epsilon}+(m_{0\sigma}\leftrightarrow m_{0\pi}), \tag{B9}$$

$$F^{(5)}=\int\frac{d^4p}{(2\pi)^4}(2\pi)^2 n_B(|p_0|)n_B(|p_0+\omega|)\,\delta(p^2-m_{0\sigma}^2)\,\delta((p+k)^2-m_{0\pi}^2). \tag{B10}$$

Here $\varepsilon=(4-n)/2$, $p^2=p_0^2-\mathbf{p}^2$, $k^2=\omega^2-\mathbf{k}^2$, and $n_B(\omega)=[e^{\omega/T}-1]^{-1}$.

The explicit forms of Eqs. (B3), (B4), (B5) for $k^2>0$ are

$$I_\phi^{(1)}=-\frac{m_{0\phi}^2}{16\pi^2}\left(\frac{1}{\varepsilon}+1-\log\frac{m_{0\phi}^2}{\kappa^2}\right), \tag{B11}$$

$$I_\phi^{(2)}=\begin{cases} -i\dfrac{1}{16\pi^2}\left[\dfrac{1}{\bar{\varepsilon}}-\log\dfrac{m_{0\phi}^2}{\kappa^2}+2+q_2\left(\log\dfrac{1-q_2}{1+q_2}+i\pi\right)\right] & \text{for } k^2>4m_{0\phi}^2, \\ -i\dfrac{1}{16\pi^2}\left[\dfrac{1}{\bar{\varepsilon}}-\log\dfrac{m_{0\phi}^2}{k^2}+2-2q_2\arctan\dfrac{1}{q_2}\right] & \text{for } 0<k^2<4m_{0\phi}^2, \end{cases} \tag{B12}$$

$$I^{(3)}=-i\frac{1}{16\pi^2}\left[\frac{1}{\bar{\varepsilon}}-\log\frac{m_{0\pi}^2}{\kappa^2}+2+\frac{k^2+m_{0\sigma}^2-m_{0\pi}^2}{2k^2}\log\frac{m_{0\pi}^2}{m_{0\sigma}^2}\right.$$
$$-\begin{cases} q_3\left(\log\dfrac{(2k^2q_3+k^2-m_{0\sigma}^2+m_{0\pi}^2)(2k^2q_3+k^2+m_{0\sigma}^2-m_{0\pi}^2)}{(2k^2q_3-k^2+m_{0\sigma}^2-m_{0\pi}^2)(2k^2q_3-k^2-m_{0\sigma}^2+m_{0\pi}^2)}-2i\pi\right) & \text{for } (m_{0\sigma}+m_{0\pi})^2<k^2, \\ 2q_3\left(\arctan\dfrac{k^2-m_{0\sigma}^2+m_{0\pi}^2}{2k^2q_3}+\arctan\dfrac{k^2+m_{0\sigma}^2-m_{0\pi}^2}{2k^2q_3}\right) & \text{for } (m_{0\sigma}-m_{0\pi})^2<k^2<(m_{0\sigma}+m_{0\pi})^2, \\ q_3\log\dfrac{(2k^2q_3+k^2-m_{0\sigma}^2+m_{0\pi}^2)(2k^2q_3+k^2+m_{0\sigma}^2-m_{0\pi}^2)}{(2k^2q_3-k^2+m_{0\sigma}^2-m_{0\pi}^2)(2k^2q_3-k^2-m_{0\sigma}^2+m_{0\pi}^2)} & \text{for } 0<k^2<(m_{0\sigma}-m_{0\pi})^2, \end{cases} \tag{B13}$$

with

$$q_2=\sqrt{\left|\frac{4m_{0\phi}^2}{k^2}-1\right|},\quad q_3=\frac{\sqrt{|(k^2+m_{0\sigma}^2-m_{0\pi}^2)^2-4k^2m_{0\sigma}^2|}}{2k^2}.$$

Equations (B6), (B7), (B8), (B9), and (B10) for $\mathbf{k}=0$ read

$$F_\phi^{(1)}=\int_0^\infty\frac{dp}{2\pi^2}\frac{p^2n_B(E(m_{0\phi}))}{E(m_{0\phi})}, \tag{B14}$$

$$F_\phi^{(2)}=i\int_0^\infty\frac{dp}{2\pi^2}\frac{p^2n_B(E(m_{0\phi}))}{E(m_{0\phi})}\frac{1}{\omega^2-4E^2(m_{0\phi})}+\theta(\omega^2-4m_{0\phi}^2)\frac{\sqrt{\omega^2-4m_{0\phi}^2}}{16\pi\omega}n_B\left(\frac{\omega}{2}\right), \tag{B15}$$

$$F_\phi^{(3)}=\theta(\omega^2-4m_{0\phi}^2)\frac{\sqrt{\omega^2-4m_{0\phi}^2}}{8\pi\omega}n_B^2\left(\frac{\omega}{2}\right), \tag{B16}$$

$$F^{(4)}=i\int_0^\infty\frac{dp}{(2\pi)^2}\frac{p^2n_B(E(m_{0\sigma}))}{E(m_{0\sigma})}\left\{\frac{1}{[\omega+E(m_{0\sigma})]^2-E(m_{0\pi})^2}+\frac{1}{[\omega-E(m_{0\sigma})]^2-E(m_{0\pi})^2}\right\}$$
$$+\left\{\begin{array}{l}\dfrac{1}{16\pi\omega^2}\sqrt{(\omega^2+m_{0\sigma}^2-m_{0\pi}^2)^2-4m_{0\sigma}^2\omega^2}\,n_B\left(\dfrac{|\omega^2+m_{0\sigma}^2-m_{0\pi}^2|}{2\omega}\right) \\ \quad [\text{for}\quad 0<\omega^2<(m_{0\sigma}-m_{0\pi})^2,(m_{0\sigma}+m_{0\pi})^2<\omega^2] \\ 0\quad [\text{for}\quad (m_{0\sigma}-m_{0\pi})^2<\omega^2<(m_{0\sigma}+m_{0\pi})^2]\end{array}\right\}+(m_{0\sigma}\leftrightarrow m_{0\pi}), \tag{B17}$$

$$F^{(5)}=\begin{cases}\dfrac{1}{8\pi\omega^2}\sqrt{(\omega^2+m_{0\sigma}^2-m_{0\pi}^2)^2-4m_{0\sigma}^2\omega^2}\,n_B\left(\dfrac{|\omega^2+m_{0\sigma}^2-m_{0\pi}^2|}{2\omega}\right)n_B\left(\dfrac{|\omega^2-m_{0\sigma}^2+m_{0\pi}^2|}{2\omega}\right) \\ \quad \text{for}\quad 0<\omega^2<(m_{0\sigma}-m_{0\pi})^2,(m_{0\sigma}+m_{0\pi})^2<\omega^2, \\ 0\quad \text{for}\quad (m_{0\sigma}-m_{0\pi})^2<\omega^2<(m_{0\sigma}+m_{0\pi})^2,\end{cases} \tag{B18}$$

where $E(m)=\sqrt{\mathbf{p}^2+m^2}$.

[1] Quark Matter '96, Nucl. Phys. **A610** (1996); Quark Matter '97, Nucl. Phys. A (to be published).

[2] LATTICE '96, Nucl. Phys. B (Proc. Suppl.) **53** (1997).

[3] A. Ukawa, Nucl. Phys. B (Proc. Suppl.) **53**, 106 (1997).

[4] See examples quoted in P. W. Anderson, *Basic Notion of Condensed Matter Physics* (Benjamin, New York, 1984); W. Gebhardt and U. Krey, *Phasenübergänge and Kritische Phänomene* (Friedr. Vieweg & Sohn, Wiesbaden, 1980).

[5] T. Hatsuda and T. Kunihiro, Phys. Rep. **247**, 221 (1994).

[6] K. Rajagopal, in *Quark-Gluon Plasma 2*, edited by R. Hwa (World Scientific, Singapore, 1995).

[7] S. Weinberg, Phys. Rev. D **9**, 3357 (1974); L. Dolan and R. Jackiw, *ibid.* **9**, 3320 (1974).

[8] D. A. Kirzhnits and A. D. Linde, Ann. Phys. (N.Y.) **101**, 195 (1976).

[9] G. Baym and G. Grinstein, Phys. Rev. D **15**, 2897 (1977); H. E. Haber and H. A. Weldon, *ibid.* **25**, 502 (1982); G. Amelino-Camelia and S.-Y. Pi, *ibid.* **47**, 2356 (1993); G. Amelino-Camelia, Nucl. Phys. **B476**, 255 (1996); Phys. Lett. B **407**, 268 (1997); H.-S. Roh and T. Matsui, Eur. Phys. J. A **1**, 205 (1998). See also H. Nakkagawa and H. Yokota, Mod. Phys. Lett. A **11**, 2259 (1996); Prog. Theor. Phys. Suppl. **129**, 209 (1997); K. Ogure and J. Sato, hep-ph/9802418 (1998) and references therein.

[10] S. Chiku and T. Hatsuda, Phys. Rev. D **57**, R6 (1998).

[11] For applications of the mean-field method to field theories, see, e.g., Y. Nambu and G. Jona-Lasinio, Phys. Rev. **122**, 345 (1961); T. Kunihiro and T. Hatsuda, Prog. Theor. Phys. **71**, 1332 (1984).

[12] Since the number of works related to OPT is enormous, we quote only two books which contain the original references: G. A. Arteca, F. M. Fernández, and E. A. Castro, *Large Order Perturbation Theory and Summation Methods in Quantum Mechanics*, (Springer-Verlag, Berlin, 1990); H. Kleinert, *Path Integrals in Quantum Mechanics, Statistical and Polymer Physics*, 2nd ed. (World Scientific, Singapore, 1995), Sec. 5. See also T. Hatsuda, T. Kunihiro, and T. Tanaka, Phys. Rev. Lett. **78**, 3229 (1997); T. Tanaka, Phys. Lett. A **238**, 79 (1998).

[13] A. Okopińska, Phys. Rev. D **36**, 2415 (1987); Mod. Phys. Lett. A **12**, 1003 (1997). [In the first reference, OPT at finite T was examined with $\mathcal{L}_I \equiv (-\lambda/4!)\phi^4 + \frac{1}{2}\chi\phi^2$ being a small perturbation, which is in contrast with our approach.] See also G. A. Hajj and P. M. Stevenson, Phys. Rev. D **37**, 413 (1988).

[14] N. Banerjee and S. Mallik, Phys. Rev. D **43**, 3368 (1991).

[15] P. Fendley, Phys. Lett. B **196**, 175 (1987).

[16] E. Braaten and R. D. Pisarski, Nucl. Phys. **B337**, 569 (1990); **B339**, 310 (1990); R. R. Parwani, Phys. Rev. D **45**, 4695 (1992); P. Arnold and C.-X. Zhai, *ibid.* **50**, 7603 (1994); **51**, 1906 (1995). See also F. Karsch, A. Patkos, and P. Petreczky, Phys. Lett. B **401**, 69 (1997).

[17] See, e.g., J. Negele and H. Orland, *Quantum Many-Particle Systems* (Addison-Wesley, New York, 1988).

[18] If we explicitly write $\hbar$ in Eq. (4), it appears as $(1/\hbar)\int_0^{\hbar/T} d^4x\mathcal{L}$. Therefore, the loop expansion by δ at finite T does not coincide with the $\hbar$ expansion. The expansion by δ should be regarded as a steepest descent evaluation of the functional integral [17].

[19] R. E. Norton and J. M. Cornwall, Ann. Phys. (N.Y.) **91**, 106 (1975); M. B. Kislinger and P. D. Morley, Phys. Rev. D **13**, 2771 (1976); H. Matsumoto, I. Ojima, and H. Umezawa, Ann. Phys. (N.Y.) **152**, 348 (1984); A. J. Niemi and G. W. Semenoff, Nucl. Phys. **B230** [FS10], 181 (1984).

[20] B. W. Lee, Nucl. Phys. **B9**, 649 (1969); *Chiral Dynamics* (Gordon and Breach, New York, 1972).

[21] T. Kugo, Prog. Theor. Phys. **57**, 593 (1977).

[22] This point was first recognized in [14].

[23] At finite T or chemical potential, only the rotational symmetry in space is preserved in the rest frame of the heat bath or matter. Therefore, $\alpha_0 \neq \alpha_1$ in general.

[24] S. Chiku and T. Hatsuda (under investigation).

[25] P. M. Stevenson, Phys. Rev. D **23**, 2916 (1981).

[26] Although $m(T)$ at high T coincides with the Debye screening mass for $\lambda \ll 1$, they could be different in higher orders: Physical Debye mass is, in general, a function of $m(T)$.

[27] In this case, $dV_L/d\varphi = \partial V_L/\partial\varphi$ at the stationary point of the thermal effective potential.

[28] W. A. Bardeen and M. Mosche, Phys. Rev. D **28**, 1372 (1983).

[29] See, e.g., C. Itzykson and J-B. Zuber, *Quantum Field Theory* (McGraw-Hill, New York, 1985); T. Muta, *Foundations of Quantum Chromodynamics* (World Scientific, Singapore, 1987).

[30] See the following papers and the references quoted therein for the breakdown of the NG theorem in self-consistent methods and for attempts to cure the problem: A. Okopińska, Phys. Lett. B **375**, 213 (1996); A. Dmitrašinović, J. A. McNeil, and J. R. Shepard, Z. Phys. C **69**, 359 (1996); G. Amelino-Camelia, Phys. Lett. B **407**, 268 (1997).

[31] T. Hatsuda and T. Kunihiro, Phys. Rev. Lett. **55**, 158 (1985); Phys. Lett. B **185**, 304 (1987); Another interesting issue is the spectral change of vector mesons: R. D. Pisarski, Phys. Lett. **110B**, 155 (1982); G. E. Brown and M. Rho, Phys. Rev. Lett. **66**, 2720 (1991); T. Hatsuda and S. H. Lee, Phys. Rev. C **46**, R34 (1992); T. Hatsuda, Y. Koike, and S. H. Lee, Nucl. Phys. **B394**, 221 (1993).

[32] H. A. Weldon, Phys. Lett. B **274**, 133 (1992); C. Song and V. Koch, *ibid.* **404**, 1 (1997).

[33] S. Huang and M. Lissia, Phys. Rev. D **52**, 1134 (1995); Phys. Lett. B **348**, 571 (1995); Phys. Rev. D **53**, 7270 (1996).

[34] L. H. Chan and R. W. Haymaker, Phys. Rev. D **7**, 402 (1973); **10**, 4170 (1974).

[35] R. D. Pisarski and F. Wilczek, Phys. Rev. D **29**, 338 (1984); K. Rajagopal and F. Wilczek, Nucl. Phys. **B399**, 395 (1993). See also M. Asakawa, Z. Huang, and X.-N. Wang, Phys. Rev. Lett. **74**, 3126 (1995); J. Randrup, Phys. Rev. D **55**, 1188 (1997) and references therein.

[36] In the present paper, A and the sign of μ^2 are defined differently from those in [34]. Also h in [34] should be considered as an unrenormalized parameter, while h in the present paper is a renormalized one.

[37] N. A. Törnqvist and M. Ross, Phys. Rev. Lett. **76**, 1575 (1996); M. Harada, F. Sannino, and J. Schechter, Phys. Rev. D **54**, 1991 (1996); Phys. Rev. Lett. **78**, 1603 (1997); S. Ishida *et al.*, Prog. Theor. Phys. **95**, 745 (1996); **98**, 1005 (1997); J. A. Oller, E. Oset, and J. R. Peláez, Phys. Rev. Lett. **80**, 3452 (1998); K. Igi and K. Hikasa, hep-ph/9807326, 1998.

[38] B. Kastening, Phys. Lett. B **283**, 287 (1992); M. Bando, T. Kugo, N. Maekawa, and H. Nakano, *ibid.* **301**, 83 (1993);

Prog. Theor. Phys. **90**, 405 (1993).

[39] M. Le Bellac, *Thermal Field Theory* (Cambridge University Press, Cambridge, England, 1996).

[40] M. Gell-Mann, R. J. Oakes, and B. Renner, Phys. Rev. **175**, 2195 (1968).

[41] D. A. Kirzhnits and A. D. Linde, Ann. Phys. (N.Y.) **101**, 195 (1976); G. Baym and G. Grinstein, Phys. Rev. D **15**, 2897 (1977); H.-S. Roh and T. Matsui, Eur. Phys. J. A **1**, 205 (1998).

[42] We have studied the free energy as a function of T near the chiral limit and found that it has a discontinuity at a certain temperature between T_1 and T_2. This is another sign that the first order nature is an artifact of the approximation. [Remember that the free energy must be a continuous function of T irrespective of the order of the phase transition: see, e.g., N. Goldenfeld, *Lectures on Phase Transitions and the Renormalization Group* (Addison-Wesley, New York, 1992).]

[43] See K. Kanaya and S. Kaya, Phys. Rev. D **51**, 2404 (1995) and references therein.

[44] H. Itoyama and A. H. Mueller, Nucl. Phys. **B218**, 349 (1983); E. V. Shuryak, Phys. Lett. B **207**, 345 (1988); J. L. Goity and H. Leutwyler, *ibid.* **228**, 517 (1989); H. Leutwyler and A. V. Smilga, Nucl. Phys. **B342**, 302 (1990); R. D. Pisarski and M. Tytgat, Phys. Rev. D **54**, 2989 (1996).

[45] A preliminary version of this study has been reported in S. Chiku, Prog. Theor. Phys. Suppl. **129**, 91 (1998).

[46] C. Gale and J. I. Kapusta, Nucl. Phys. **B357**, 65 (1991).

[47] S. Hafjitheodoridis and B. Moussallam, Phys. Rev. D **37**, 1331 (1988).

[48] S. P. Klevansky, Nucl. Phys. **A575**, 605 (1994).

[49] P. Rehberg, Yu. I. Kalinovskii, and D. Blaschke, Nucl. Phys. **A622**, 478 (1997). In this paper, the mode couplings are not taken into account.

[50] A. D. Linde, Phys. Lett. **96B**, 289 (1980). See also T. Hatsuda, Phys. Rev. D **56**, 8111 (1997) and references therein.